Geochemical Perspectives Letters EAG

Iron isotopic evidence for growth of continental crust at convergent margins

Y. He, R.L. Rudnick, F.-Z. Teng, H. Wu, S. Ke

Supplementary Information

The Supplementary Information includes:

- Geological Settings of the Underplating Mafic Magmas Beneath McBride and Chudleigh
- Monte Carlo Simulations
- Iron Isotope Composition of the Upper Continental Crust
- Iron Isotope Fractionation During Intracrustal Differentiation
- Iron Isotope Fractionation During the Formation of Intraplate Felsic Magmas with 'Arc-Like' Trace-Element Signature
- Constraining the Proportion of Continental Growth in Convergent Margins from the Fe Isotope Perspective
- Tables S-1 to S-6
- Figures S-1 and S-5
- Supplementary Information References

Geological Settings of the Underplating Mafic Magmas Beneath McBride and Chudleigh

Late Paleozoic (from ~ 320 to 220 Ma) zircons, related to crustal anatexis and granulite metamorphism, have been found in all the zircon-bearing McBride xenoliths (Rudnick and Williams, 1987). Intensive heating of the lower continental crust by mantle-derived mafic melts thus likely occurred in the late Paleozoic. Granulite xenoliths with metasedimentary protoliths suggest burial of supercrustal rocks into the lower crust. These features, along with extensive calc-alkaline felsic magmatism on the surface, are consistent with basaltic underplating and reworking of preexisting crust in a continental arc setting (Rudnick and Williams, 1987; Rudnick, 1990). The geodynamic context of the underplating magmas beneath Chudleigh, however, is unknown, because of the lack of precise age data for these rocks. Based on the correlation coefficient (r) between $\varepsilon_{Nd}(t)$ and Mg# for Chudleigh xenoliths, which is 0.91 at t = 0 and decreases with increasing age, Rudnick *et al.* (1986) suggested that the xenolith suite is relatively young (<100 Ma). Most <100 Ma basalts from northern Queensland erupted in an intraplate setting and have high Nb/La ratios (Shea *et al.*, 2022). The low Nb/La feature of Chudleigh xenoliths is consistent with their cumulate origin, as the dominant crystallizing phases are pyroxenes and plagioclase that both have D_{Nb}/D_{La} << 1 (Bindeman *et al.*, 1998; Wood and Trigila, 2001; Adam and Green, 2006).

Monte Carlo Simulations

The mean Fe isotope compositions of Chudleigh and McBride xenoliths, as well as the lower continental crust, were calculated as $\overline{\delta^{56}\mathrm{Fe}} = \sum w_i \cdot \delta^{56}\mathrm{Fe}_i$, where $w_i = [\mathrm{FeO_t}]_i / \sum [\mathrm{FeO_t}]_i$. The uncertainties of the mean values were obtained from these Monte Carlo simulations. The mean δ^{56}Fe was calculated with that of each sample randomly generated following a normal distribution of $\delta^{56}\mathrm{Fe}_{measured} \pm 2\sigma$. The calculation was repeated 10^5 times, and then the propagated uncertainties for the mean δ^{56}Fe were calculated. The same method was also used to constrain the propagated uncertainties of mean δ^{56}Fe of the continental crust and the proportion of the continent growth contributed by convergent margins.

Iron Isotope Composition of the Upper Continental Crust

The mean Fe isotope composition of the upper continental crust has been estimated here following the strategy of Poitrasson (2006), by averaging the low-Si intermediate-felsic igneous rocks and high-Si granitic rocks with the proportions given by Wedepohl *et al.* (1995). Compared to the limited database in Poitrasson (2006), our estimate includes Fe isotopic data for 360 intermediate-felsic igneous rocks compiled from the literature (Table S-4), and suggests a mean δ^{56}Fe value of 0.109 ± 0.008 ‰ (2se) for the upper continental crust, consistent with previous studies (Foden *et al.*, 2015; Liu *et al.*, 2022).

Iron Isotope Fractionation During Intracrustal Differentiation

Compared to the limited localities where lower crustal xenoliths are available for analysis, the upper continental crust is readily accessible, and its mean δ^{56}Fe has been well constrained to be ~0.109 ‰ (Foden *et al.*, 2015; Liu *et al.*, 2022; this study). In addition to the xenolith analyses presented here, the mean δ^{56}Fe of the lower continental crust can be independently constrained from that of the upper continental crust if isotope fractionation during intracrustal differentiation is known. Here, we assume the upper and lower continental crust are complementary to each and related by crustal anatexis. Iron isotope fractionation during crustal anatexis has been previously studied by measurements on migmatites from the Black Hills region of South Dakota, USA (Telus *et al.*, 2012) and the Dabie orogen, China (Xu *et al.*, 2017). The protoliths of the Black Hills migmatites are schists, with melanosomes dominated by biotite and sillimanite, while the protoliths of Dabie migmatites are orthogneisses, and the melting reaction is inferred to be biotite + plagioclase + quartz + fluid —> granitic melt + amphibole + residual plagioclase (Wang *et al.*, 2013). After excluding the samples that have likely been affected by plagioclase accumulation and the presence of peritectic amphibole in the leucosome, eight leucosome-melanosome pairs yield a mean $\Delta^{56}Fe_{melt-residue}$ of 0.078 ± 0.019 ‰ (2se). This value was taken as a maximum estimate for $\Delta^{56}Fe_{melt-residue}$ during intracrustal differentiation, as the leucosomes have SiO_2 (72.5 ~ 79.5 wt. %) and (Na+K)/(Ca+Mg) (1.17 ~ 8.62) both systematically higher than the upper continental crust (~66 wt. % and 1.31; Rudnick and Gao, 2014). Mean force constants of Fe-O bonds in silicate glasses and global granitoid data both suggest a higher $\Delta^{56}Fe_{melt-solid}$ for a melt with higher SiO_2 and (Na+K)/(Ca+Mg), if the other parameters remain constant. Two leucosome-melanosome pairs, with (Na+K)/(Ca+Mg) of the leucosomes (1.17 and 1.57), analogous to that of the upper continental crust, indeed have a much lower $\Delta^{56}Fe_{melt-residue}$ of 0.045 ± 0.017 ‰ (2se). One may argue that differentiation of the continental crust also involves partial melting of mafic lithologies at depths. Iron isotope fractionation during partial melting of a thickened mafic lower crust, leaving a garnet + clinopyroxene residue, has been constrained by measurements on low-Mg adakitic rocks from the Dabie orogen (He *et al.*, 2017). When compared with local eclogites, $\Delta^{56}Fe_{melt-residue}$ is estimated and varies from 0.021‰ to 0.163 ‰, positively correlated to the melt $(Dy/Yb)_N$ (i.e., $\Delta^{56}Fe_{melt-residue} = 0.036 \times (Dy/Yb)_N + 0.004$, $R^2 = 0.44$). This is consistent with available fractionation factors showing that garnet is isotopically lighter than the co-existing clinopyroxene and melt; more residual garnet in the source tends to enhance $\Delta^{56}Fe_{melt-residue}$ (He *et al.*, 2017). According to the equation, a $\Delta^{56}Fe_{melt-residue}$ of ~0.051 ‰ is preferred for a melt derived from mafic lithologies with a composition analogous to the upper continental crust with a $(Dy/Yb)_N$ ~1.33 (Rudnick and Gao, 2014). In summary, to the best of our knowledge, the $\delta^{56}Fe$ difference between the upper and lower continental crust could range from ~0.045 ‰ to ~0.078 ‰; the lower continental crust is thus expected to have a mean $\delta^{56}Fe$ between 0.03 ‰ and 0.07 ‰.

Iron Isotope Fractionation During the Formation of Intraplate Felsic Magmas with 'Arc-Like' Trace-Element Signatures

To the best of our knowledge, no Fe isotopic data has been reported for felsic magmas with 'arc-like' trace elemental patterns from intraplate settings. Such magmas can be generated by partial melting of basaltic crust with residual Ti-rich minerals, e.g., hornblende, rutile and ilmenite, and may have further experienced fractional crystallization of ilmenite-bearing assemblages (e.g., Smithes *et al.*, 2009; Willbold *et al.*, 2009; Johnson *et al.*, 2017). Both mafic silicates and ilmentite are isotopically lighter than their co-existing melts (Polyakov and Mineev, 2000; Dauphas *et al.*, 2014; He *et al.*, 2017; Sossi and O'Neil, 2017). Thus, felsic magmas with 'arc-like' trace elemental patterns from intraplate settings are expected to have $\delta^{56}Fe$ values higher than parental intraplate basalts, represented by OIB that have an average $\delta^{56}Fe$ of 0.146 ± 0.012 ‰ (2se; Table S-3).

Constraining the Proportion of Continental Growth in Convergent Margins from the Fe Isotope Perspective

Basaltic magmas at convergent margins and intraplate settings are likely the dominant juvenile materials responsible for continental growth, therefore, the average composition of primitive building materials of continental crust (i.e., $\delta^{56}Fe_{CC0}$) can be described by mass balance:

$$\delta^{56}Fe_{CC0} = \frac{\delta^{56}Fe_{CM}\cdot[FeOt]_{CM}\cdot f_{CM} + \delta^{56}Fe_{IS}\cdot[FeOt]_{IS}\cdot(1-f_{CM})}{[FeOt]_{CM}\cdot f_{CM} + [FeOt]_{IS}\cdot(1-f_{CM})} \quad \text{(S-1)}$$

where CM and IS are abbreviations of convergent margins and intraplate settings. $\delta^{56}Fe_{CM}$, $[FeO_t]_{CM}$, $\delta^{56}Fe_{IS}$, and $[FeO_t]_{IS}$ can be represented by the mean compositions of arc basalts and oceanic island basalts (Table S-3). The equation (1) can be rearranged to:

$$f_{CM} = \frac{\delta^{56}Fe_{IS}\cdot[FeOt]_{IS} - \delta^{56}Fe_{CC0}\cdot[FeOt]_{IS}}{(\delta^{56}Fe_{IS} - \delta^{56}Fe_{CC0})\cdot[FeOt]_{IS} - (\delta^{56}Fe_{CM} - \delta^{56}Fe_{CC0})\cdot[FeOt]_{CM}} \quad \text{(S-2)}$$

$\delta^{56}Fe_{CC0}$ is unknown, as the continental crust has evolved from its primitive building materials to an andesitic composition (Rudnick, 1995; Rudnick and Gao, 2014), mainly through density foundering of mafic cumulates or residua at the base of the crust if they convert to eclogite (*e.g.*, Kay and Kay, 1993), or through loss of these dense mafic rocks during continental subduction followed by relamination of the less dense portions of the subducted crust (Hacker *et al.*, 2011). Lighter Fe isotopes are concentrated in the residua during crustal melting (Telus *et al.*, 2012; He *et al.*, 2017; Xu *et al.*, 2017), and are also enriched in mafic cumulates during magma differentiation, except that magnetite becomes an abundant crystalline phase (e.g., Teng *et al.*, 2008; Sossi *et al.*, 2012; Du *et al.*, 2022). Removal of magnetite could be less important than mafic minerals, as the continental crust has a Mg# ~ 55.3, which is lower than primitive basalts (Rudnick and Gao, 2014). The mean $\delta^{56}Fe$ of the continental crust (*i.e.*, $\delta^{56}Fe_{CC}$) thus provides an upper limit for $\delta^{56}Fe_{CC0}$; replacing $\delta^{56}Fe_{CC0}$ by $\delta^{56}Fe_{CC}$ in the equation (2) can provide a minimum estimate of f_{CM}.

Supplementary Tables

Table S-1 Iron isotopic compositions of the Chudleigh and McBride xenoliths from North Queensland, Australia.
Table S-2 Iron isotopic budget of the continental crust.
Table S-3 Iron isotopic compositions of representative least differentiated basalts.
Table S-4 Fe isotopic data of global intermediate-felsic igneous magmas reported in the literature.
Table S-5 Fe isotopic data of representative Archean TTG reported in the literature.
Table S-6 Compiled elemental and isotopic data available for the Chudleigh and McBride xenoliths.

Tables S-1 to S-6 are available for download (.xlsx) from the online version of this article at https://doi.org/10.7185/geochemlet.2542.

Supplementary Figures

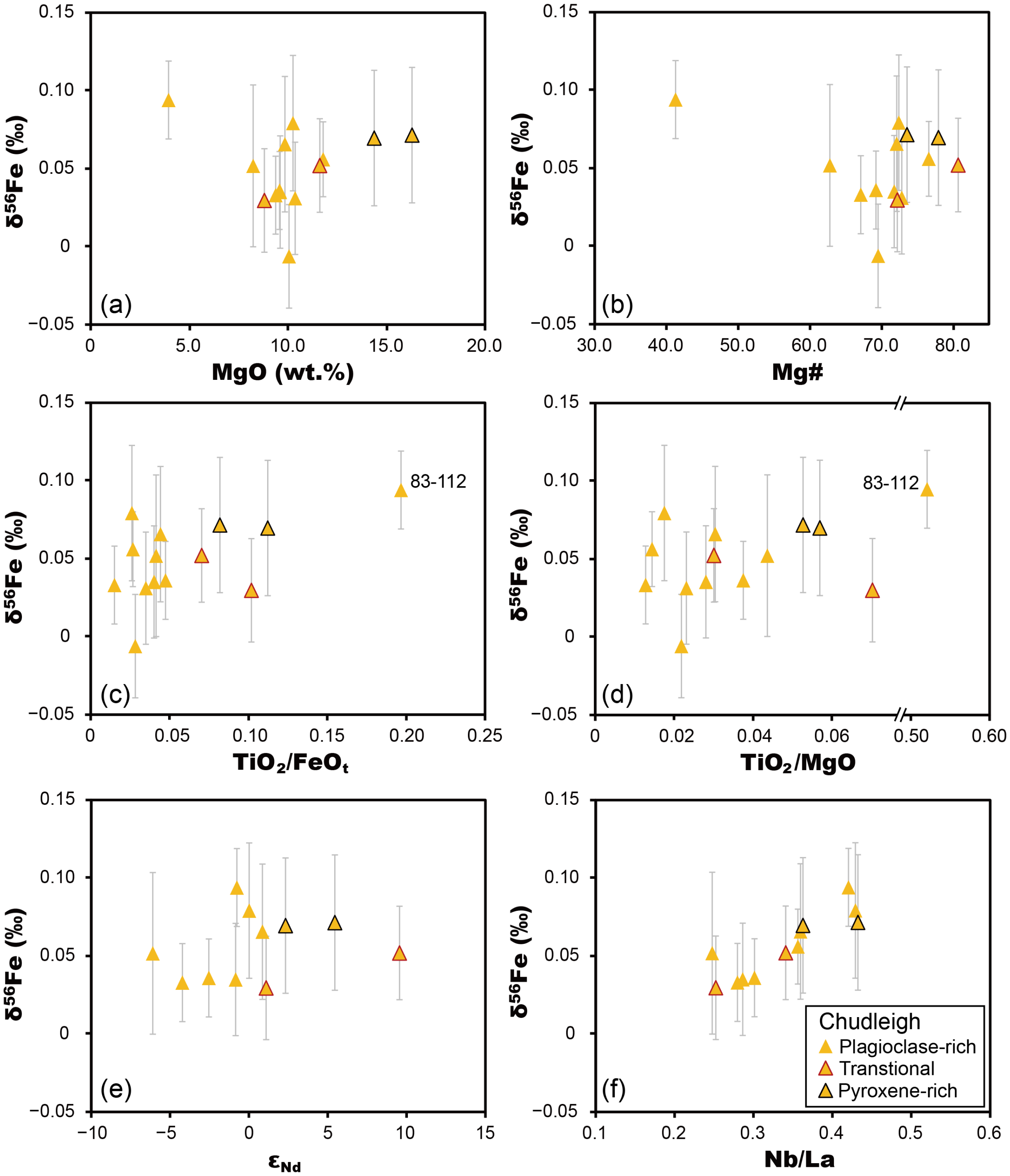

Figure S-1 Plots of δ^{56}Fe versus MgO (a), Mg# (b), TiO_2/FeO_t (c), TiO_2/MgO (d), ε_{Nd} (e) and Nb/La (f) for Chudleigh mafic granulite xenoliths. Elemental and Nd isotopic data are from Rudnick *et al.* (1986).

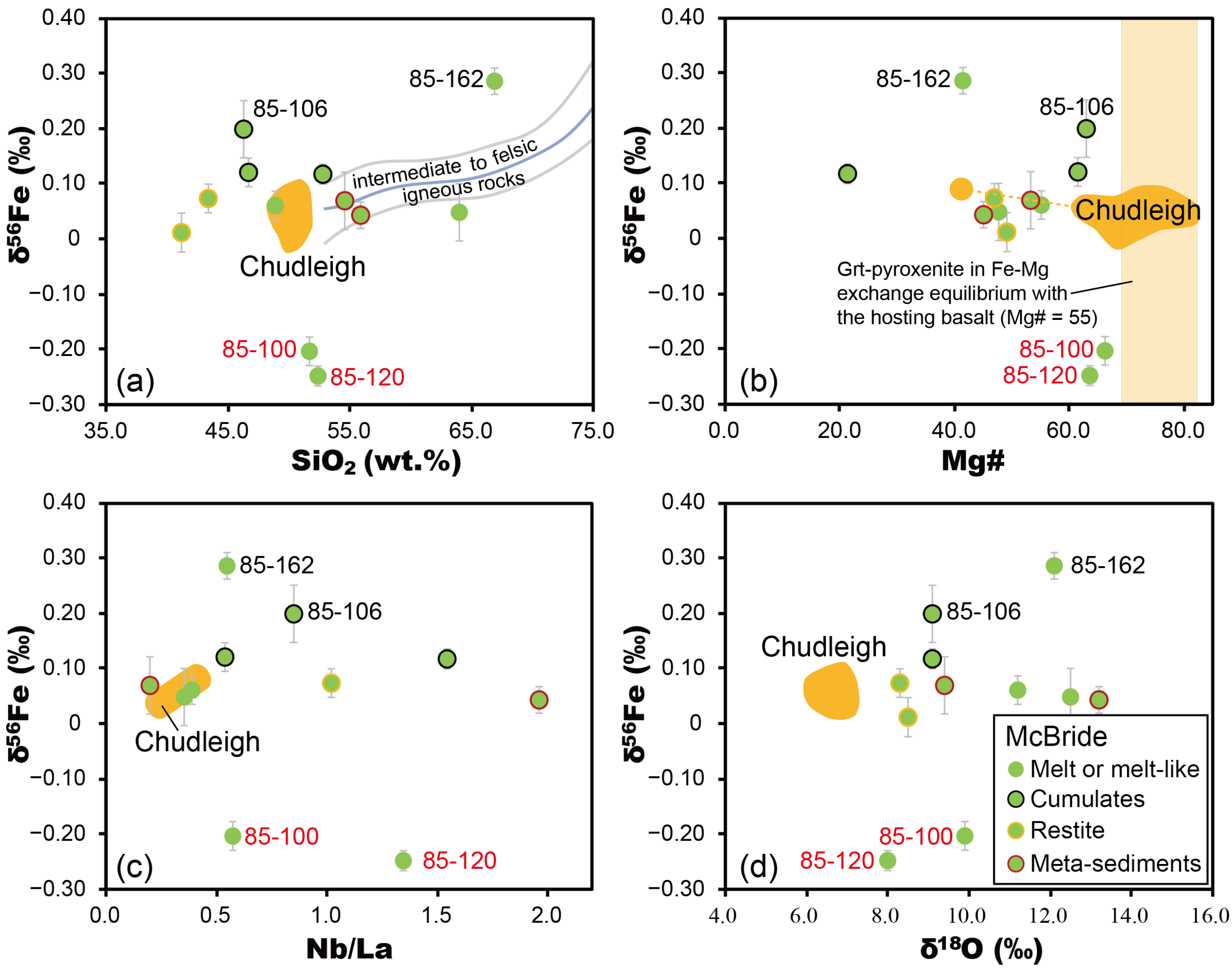

Figure S-2 Plots of δ^{56}Fe versus SiO_2 **(a)**, Mg# **(b)**, Nb/La **(c)** and δ^{18}O **(d)** for xenoliths from McBride. Elemental and O isotopic data for McBride are from Rudnick and Taylor (1987) and Kempton and Harmon (1992), respectively; data for Chudleigh are from Rudnick *et al.* (1986) and Kempton and Harmon (1992), respectively. Local weighted regression (LOESS) of intermediate to felsic igneous rocks compiled in Table S-4 and Table S-5 with a SiO_2 bandwidth of 1.0 wt. % as well as those for the upper and lower half samples have been shown for comparison. Samples likely affected by Fe-Mg inter-diffusion are denoted with sample numbers. The Mg# range is outlined for garnet and clinopyroxenes in Fe-Mg exchange equilibrium with the hosting basalt (Mg# = 55, Irving and Frey, 1984), using a Kd(Fe-Mg) estimated from experimental runs of Petermann and Hirschmann (2003).

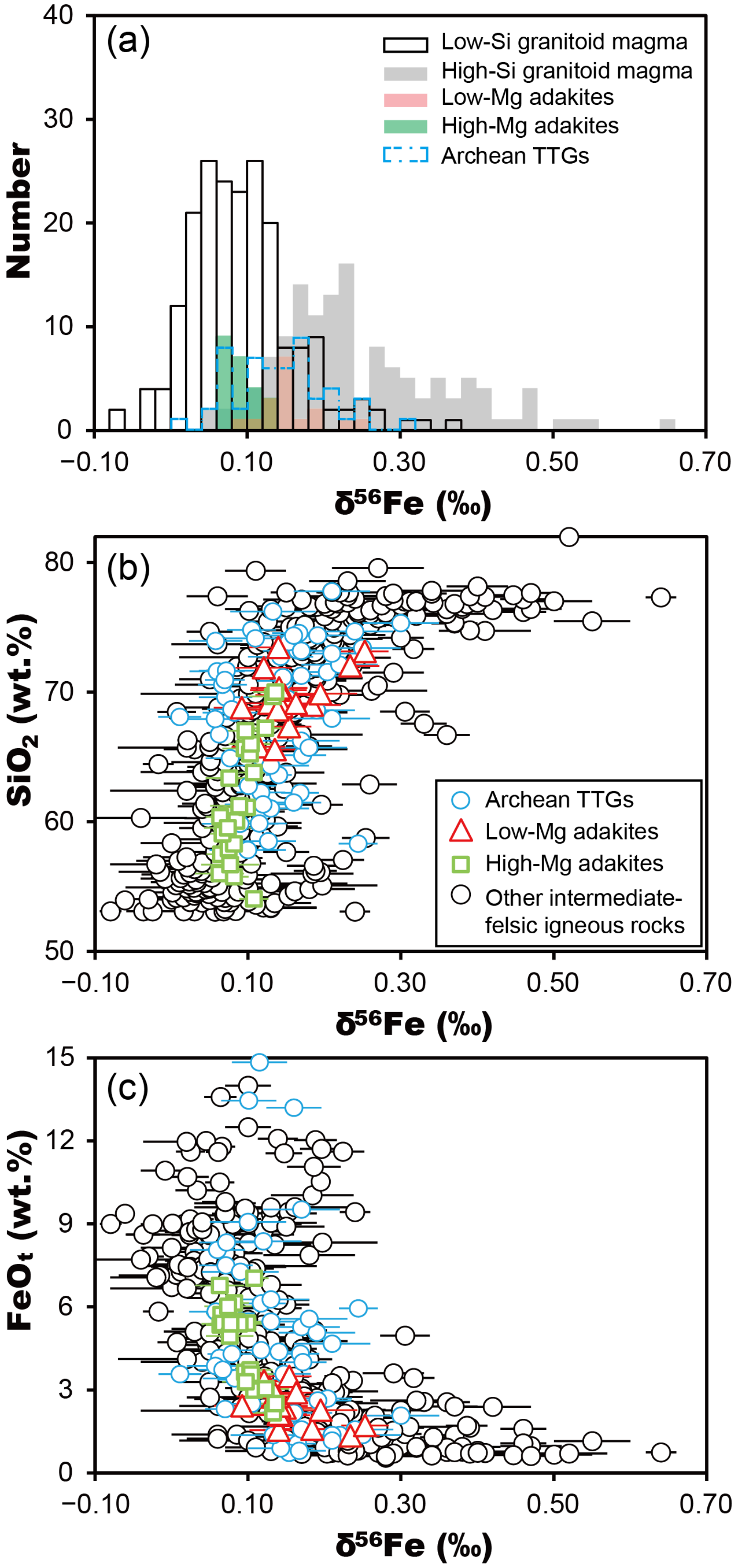

Figure S-3 δ^{56}Fe of global intermediate-felsic igneous rocks **(a)** and correlations with SiO_2 and FeO_t **(b-c)**. Data are compiled in Table S-4 and Table S-5. Except for adakites and TTGs, the other samples are grouped into low-Si and high-Si granitoid magmas in (a) by $SiO_2 < 71$ wt. % and $\geqslant 71$ wt. % respectively (Poitrasson and Freydier, 2005).

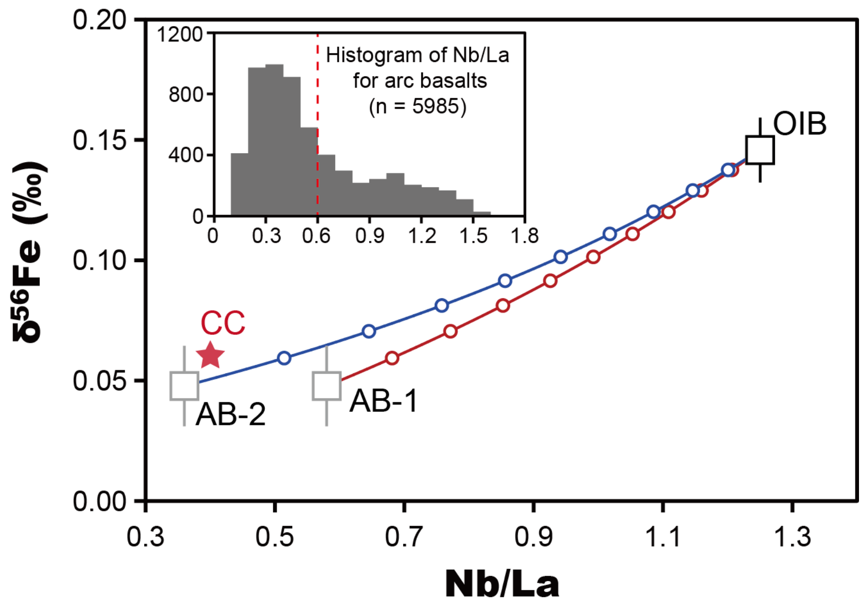

Figure S-4 Plot of $\delta^{56}Fe$ versus Nb/La illustrating the mixing between OIB and arc basalts (AB). Iron isotope compositions of continental crust (CC), OIB and arc basalts are compiled in this study (Table S-2 and Table S-3). Open circles denote 10 % increments of mixing. Elemental composition of the continental crust is from Rudnick and Gao (2003). Nb and La contents of mean OIB and arc basalts are compiled from GeoRoc (https://georoc.mpch-mainz.gwdg.de//georoc/). Only volcanic whole rock data with MgO between 6.0 wt. % and 12.0 wt. % were included for ocean islands and convergent margins - arcs. Samples with highest (>95 %) and lowest (<5 %) Nb/La were excluded to avoid possibly erroneous data. With these filters, 4912 OIB yield a mean composition of 35.5 ± 0.8 (2 sigma, if not specified) ppm Nb, 28.3 ± 0.6 ppm La and a Nb/La of 1.25 ± 0.01; 5985 arc basalts yield a mean composition with 11.5 ± 0.5 ppm Nb, 17.7 ± 0.6 ppm La and a Nb/La of 0.58 ± 0.01 (shown as "AB-1"). For a comparison, mean Nb/La was previously estimated to be ~0.57, ~0.53 and ~1.30 for island arc basalts, continental arc basalts, and OIB, respectively (Sun and McDonough, 1989; Kelemen *et al.*, 2014). The continental crust has a Nb/La lower than AB-1, suggesting a more important role for low Nb/La arc basalts in building continental crust (e.g., AB-2 (Nb/La ~ 0.36, n = 3859), with an additional filter of Nb/La ≤ 0.6 as shown in the insert), and/or reflecting density foundering of high Nb/La mafic cumulates or residua containing Ti-bearing minerals (*e.g.*, ilmenite and rutile) (e.g., Kay and Kay, 1993; Rudnick, 1995; He *et al.*, 2011). Nonetheless, both Fe isotope data and the Nb-La budget of the continental crust indicate its growth dominantly at convergent margins.

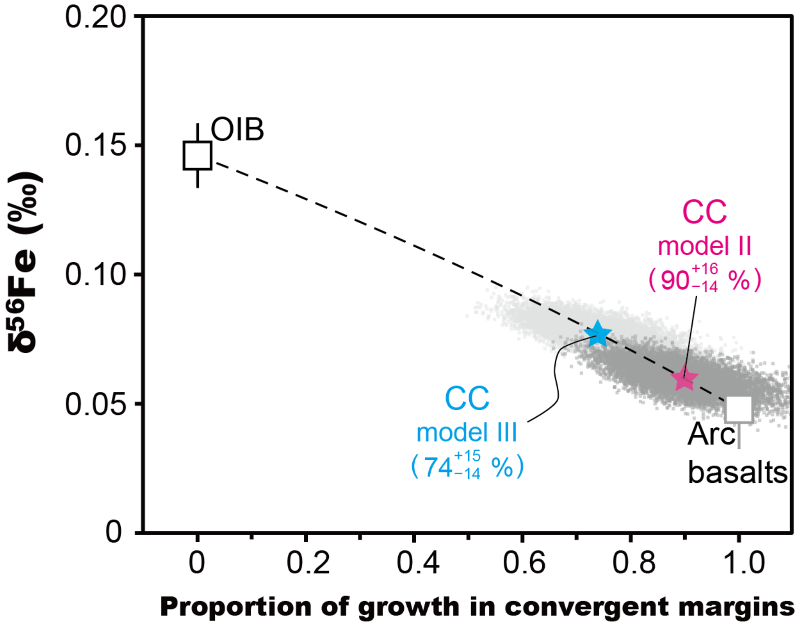

Figure S-5 Proportion of continental crustal growth at convergent margins (i.e., f_{CM}) estimated by different continental crust (CC) models. With a purpose to evaluate the robustness of the estimated f_{CM}, we set up two extra CC models in the perspective of Fe isotope budget. Compared to the model CC in the main text (model I), the model II adopts a larger uncertainty of the mean δ^{56}Fe of LCC (i.e., ± 0.02 ‰ based on the discussion in Supplementary Information: Iron isotope fractionation during intracrustal differentiation). In model III, we consider that the MCC might have a δ^{56}Fe higher than, instead of equal to, the LCC, and set its mean δ^{56}Fe as that of the UCC for a maximum estimate, providing that the MCC has a more evolved elemental composition compared to the LCC. The enlarged δ^{56}Fe uncertainty (i.e., that used in model II) was also adopted for mean LCC in the model III. The model II and III yield mean δ^{56}Fe of the CC as 0.060 ± 0.011 ‰ (2se) and 0.077 ± 0.010 ‰ (2se), respectively. With these modifications, the according f_{CM} was then calculated by Monte Carlo method and shown as described in Fig.3. All these practices convince the idea that the continental crust growth has predominantly occurred at convergent margins through arc basaltic magmatism, while future analyses on more MCC and LCC samples from other localities are called on to refine our knowledge about the Fe isotope budget of the CC.

Supplementary Information References

Adam, J., Green, T. (2006) Trace element partitioning between mica- and amphibole-bearing garnet lherzolite and hydrous basanitic melt: 1. Experimental results and the investigation of controls on partitioning behaviour. *Contributions to Mineralogy and Petrology* 152, 1–17. https://doi.org/10.1007/s00410-006-0085-4

Bindeman, I.N., Davis, A.M., Drake, M.J. (1998) Ion microprobe study of plagioclase-basalt partition experiments at natural concentration levels of trace elements. *Geochimica et Cosmochimica Acta* 62, 1175–1193. https://doi.org/10.1016/S0016-7037(98)00047-7

Dauphas, N., Roskosz, M., Alp, E.E., Neuville, D.R., Hu, M.Y., Sio, C.K., Tissot, F.L.H., Zhao, J., Tissandier, L., Médard, E., Cordier, C. (2014) Magma redox and structural controls on iron isotope variations in Earth's mantle and crust. *Earth and Planetary Science Letters* 398, 127–140. https://doi.org/10.1016/j.epsl.2014.04.033

Du, D.H., Tang, M., Li, W.Q., Kay, S.M., Wang, X.L. (2022) What drives Fe depletion in calc-alkaline magma differentiation: insights from Fe isotopes. *Geology* 50, 552–556. https://doi.org/10.1130/G49705.1

Foden, J., Sossi, P.A., Wawryk, C.M. (2015) Fe isotopes and the contrasting petrogenesis of A-, I- and S-type granite. *Lithos* 212–215, 32–44. https://doi.org/10.1016/j.lithos.2014.10.015

Hacker, B.R., Kelemen, P.B., Behn, M.D. (2011) Differentiation of the continental crust by relamination. *Earth and Planetary Science Letters* 307, 501–516. https://doi.org/10.1016/j.epsl.2011.05.024

He, Y., Li, S., Hoefs, J., Huang, F., Liu, S.A., Hou, Z. (2011) Post-collisional granitoids from the Dabie orogen: New evidence for partial melting of a thickened continental crust. *Geochimica et Cosmochimica Acta* 75, 3815–3838. https://doi.org/10.1016/j.gca.2011.04.011

He, Y., Wu, H., Ke, S., Liu, S.A., Wang, Q. (2017) Iron isotopic compositions of adakitic and non-adakitic granitic magmas: Magma compositional control and subtle residual garnet effect. *Geochimica et Cosmochimica Acta* 203, 89–102. https://doi.org/10.1016/j.gca.2017.01.005

Irving, A.J., Frey, F.A. (1984) Trace element abundances in megacrysts and their host basalts: Constraints on partition coefficients and megacryst genesis. *Geochemica et Cosmochimica Acta* 48, 1201–1221. https://doi.org/10.1016/0016-7037(84)90056-5

Johnson, T.E., Brown, M., Gardiner, N.J., Kirkland, C.L., Smithies, R.H. (2017) Earth's first stable continents did not form by subduction. *Nature* 543, 239–242. https://doi.org/10.1038/nature21383

Kay, R.W., Kay, S.M. (1993) Delamination and delamination magmatism. *Tectonophysics* 219, 177–189. https://doi.org/10.1016/0040-1951(93)90295-U

Kelemen, P.B., Hanghøj, K., Greene, A.R. (2014) 4.21 - One View of the Geochemistry of Subduction-Related Magmatic Arcs, with an Emphasis on Primitive Andesite and Lower Crust. In: Holland, H.D., Turekian, K.K. (Eds.) *Treatise on Geochemistry.* Second Edition, Elsevier, Oxford, 749–806. https://doi.org/10.1016/B978-0-08-095975-7.00323-5

Kempton, P.D., Harmon, R.S. (1992) Oxygen isotope evidence for large-scale hybridization of the lower crust during magmatic underplating. *Geochimica et Cosmochimica Acta* 56, 971–986. https://doi.org/10.1016/0016-7037(92)90041-G

Liu, X.M., Gaschnig, R.M., Rudnick, R.L., Hazen, R.M., Shahar, A. (2022) Constant iron isotope composition of the upper continental crust over the past 3 Gyr. *Geochemical Perspectives Letters* 22, 16–19. https://doi.org/10.7185/geochemlet.2221

Pertermann, M., Hirschmann, M.M. (2003) Anhydrous partial melting experiments on MORB-like eclogite: phase relations, phase compositions and mineral-melt partitioning of major elements at 2–3 GPa. *Journal of Petrology* 44, 2173–2201. https://doi.org/10.1093/petrology/egg074

Poitrasson, F. (2006) On the iron isotope homogeneity level of the continental crust. *Chemical Geology* 235, 195–200. https://doi.org/10.1016/j.chemgeo.2006.06.010

Poitrasson, F., Freydier, R. (2005) Heavy iron isotope composition of granites determined by high resolution MC-ICP-MS. *Chemical Geology* 222, 132–147. https://doi.org/10.1016/j.chemgeo.2005.07.005

Polyakov, V.B., Mineev, S.D. (2000) The use of Mössbauer spectroscopy in stable isotope geochemistry. *Geochimica et Cosmochimica Acta* 64, 849–865. https://doi.org/10.1016/S0016-7037(99)00329-4

Rudnick, R.L. (1990) Nd and Sr isotopic compositions of lower-crustal xenoliths from north Queensland, Australia: Implications for Nd model ages and crustal growth processes. *Chemical Geology* 83, 195–208. https://doi.org/10.1016/0009-2541(90)90280-K

Rudnick, R.L. (1995) Making continental crust. *Nature* 378, 571–578. https://doi.org/10.1038/378571a0

Rudnick, R.L., Gao, S. (2014) 4.1 - Composition of the Continental Crust. In: Holland, H.D., Turekian, K.K. (Eds.) *Treatise on Geochemistry.* Second Edition, Elsevier, Oxford, 1–51. https://doi.org/10.1016/B978-0-08-095975-7.00301-6

Rudnick, R.L., Taylor, S.R. (1987) The composition and petrogenesis of the lower crust: a xenolith study. *Journal of Geophysical Research* 92, 13981–14005. https://doi.org/10.1029/JB092iB13p13981

Rudnick, R.L., Williams, I.S. (1987) Dating the lower crust by ion microprobe. *Earth and Planetary Science Letters* 85, 145–161. https://doi.org/10.1016/0012-821X(87)90028-8

Rudnick, R.L., McDonough, W.F., McCulloch, M.T., Taylor, S.R. (1986) Lower crustal xenoliths from Queensland, Australia: Evidence for deep crustal assimilation and fractionation of continental basalts. *Geochemica et Cosmochimica Acta* 50, 1099–1115. https://doi.org/10.1016/0016-7037(86)90391-1

Shea, J.J., Ezad, I.S., Foley, S.F., Lanati, A.W. (2022) The eastern Australian volcanic province, its primitive melts, constraints on melt sources and the influence of mantle metasomatism. *Earth-Science Reviews* 233, 104168. https://doi.org/10.1016/j.earscirev.2022.104168

Smithies, R.H., Champion, D.C., Van Kranendonk, M.J. (2009) Formation of Paleoarchean continental crust through infracrustal melting of enriched basalt. *Earth and Planetary Science Letters* 281, 298–306. https://doi.org/10.1016/j.epsl.2009.03.003

Sossi, P.A., Foden, J.D., Halverson, G.P. (2012) Redox-controlled iron isotope fractionation during magmatic differentiation: an example from the Red Hill intrusion, S. Tasmania. *Contributions to Mineralogy and Petrology* 164, 757–772. https://doi.org/10.1007/s00410-012-0769-x

Sossi, P.A., O'Neill, H.St.C. (2017) The effect of bonding environment on iron isotope fractionation between minerals at high temperature. *Geochimica et Cosmochimica Acta* 196, 121–143. https://doi.org/10.1016/j.gca.2016.09.017

Sun, S.-s., McDonough, W.F. (1989) Chemical and isotopic systematics of oceanic basalts: Implications for mantle composition and processes. *Geological Society, London, Special Publications* 42, 313–345. https://doi.org/10.1144/GSL.SP.1989.042.01.19

Telus, M., Dauphas, N., Moynier, F., Tissot, F.L.H., Teng, F.-Z., Nabelek, P.I., Craddock, P.R., Groat, L.A. (2012) Iron, zinc, magnesium and uranium isotopic fractionation during continental crust differentiation: the tale from migmatites, granitoids, and pegmatites. *Geochimica et Cosmochimica Acta* 97, 247–265. https://doi.org/10.1016/j.gca.2012.08.024

Teng, F.-Z., Dauphas, N., Helz, R.T. (2008) Iron isotope fractionation during magmatic differentiation in Kilauea Iki lava lake. *Science* 320, 1620–1622. https://doi.org/10.1126/science.1157166

Wang, S.J., Li, S.J., Chen, L.J., He, Y.S., An, S.C., Shen, J. (2013) Geochronology and geochemistry of leucosomes in the North Dabie Terrane, East China: implication for post-UHPM crustal melting during exhumation. *Contributions to Mineralogy and Petrology* 165, 1009–1029. https://doi.org/10.1007/s00410-012-0845-2

Wedepohl, K.H. (1995) The composition of the continental crust. *Geochimica et Cosmochimica Acta* 59, 1217–1232. https://doi.org/10.1016/0016-7037(95)00038-2

Willbold, M., Hegner, E., Stracke, A., Rocholl, A. (2009) Continental geochemical signatures in dacites from Iceland and implications for models of early Archean crust formation. *Earth and Planetary Science Letters* 279, 44–52. https://doi.org/10.1016/j.epsl.2008.12.029

Wood, B.J., Trigila, R. (2001) Experimental determination of aluminous clinopyroxene-melt partition coefficients for potassic liquids, with application to the evolution of the Roman province potassic magmas. *Chemical Geology* 172, 213–223. https://doi.org/10.1016/S0009-2541(00)00259-X

Xu, L.J., He, Y., Wang, S.J., Wu, H., Li, S. (2017) Iron isotope fractionation during crustal anatexis: Constraints from migmatites from the Dabie orogen, Central China. *Lithos* 284–285, 171–179. https://doi.org/10.1016/j.lithos.2017.04.005